Spatial-Temporal Three-Corned Hat for Soil Moisture Uncertainty Evaluation Over the Qinghai-Tibet Plateau

Ling Zhang[1,a], Yongxu Wang[2,3,c*], Zhaohui Xue[2,3,b*]

[a]zhangling_jmi@163.com, [b*] zhaohui.xue@hhu.edu.cn, [c*]wyx05242021@163.com

[1]School of Naval Architecture & Ocean Engineering, Jiangsu Maritime Institute, Nanjing, 211100, China
[2]School of Earth Sciences and Engineering, Hohai University, Nanjing, 211100, China
[3]Jiangsu Province Engineering Research Center of Water Resources and Environment Assessment Using Remote Sensing, Hohai University, Nanjing, 211100, China

Abstract: Accurate uncertainty evaluation of soil moisture (SM) products is crucial for maximizing their utility in research and applications in hydro-meteorology and climatology. At present, the uncertainty analysis of SM is mostly carried out from the perspective of temporal domain based on time series. Whereas, the influence of spatial heterogeneity when representing spatial errors is usually ignored. To solve this problem, a novel spatial-temporal three-corned hat (ST-TCH) method is proposed for SM uncertainty evaluation. Firstly, a moving window is used to construct the spatial-temporal data cube of SM within the neighborhood. Secondly, the heterogeneous pixels are eliminated based on Spearman correlation coefficient to avoid the interference of heterogeneous pixels. Finally, the 3D spatial-temporal data is vectorized into a sequence which is fed into TCH to produce the relative uncertainty (RU). Experiments are conducted on four SM products over the Qinghai-Tibet plateau (QTP). To quantitatively verify the performance, four products are merged based on the estimated RU, and the merged products are further validated with the in-situ data. Results demonstrate that RU obtained by ST-TCH is more complete in spatial distribution, and the merged product produced by ST-TCH is more close to the in-situ data with R = 0.769 among all products.

Index Terms—Soil moisture (SM); three-corned hat (TCH); spatial-temporal fusion, Qinghai-Tibet Plateau (QTP).

1. Introduction

SOIL moisture is an crucial climate variable in hydro-meteorological and climate[1]. Although SM products from multi-source are now widely available, many of them are associated with varying degrees of uncertainty[2]. Quantifying the uncertainty of various soil moisture products is a prerequisite for their utilization. At present, the uncertainty quantification methods of soil moisture products mainly include direct evaluation and indirect evaluation[3].

Direct evaluation is to compare the soil moisture products with the in-situ data to find out the statistical error. Statistical variables commonly used in direct evaluation mainly include Pearson correlation coefficient (R), root mean square error (RMSE), deviation and unbiased root mean square error (unbias)[4]. However, the direct evaluation based on in-situ data is

IDEE 2023, November 24-26, Zhengzhou, People's Republic of China

DOI 10.4108/eai.24-11-2023.2343429

limited to the discrete network of measured stations and can not be extended to areas without high-density measured stations.

Indirect evaluation methods mainly include Triple Collocation (TC)[5-8], Extended Triple Collocation (ETC) [9], the three-cornered hat (TCH)[3,10,11], Quadruple Collocation (QC)[12], etc. Wang Shuguo et al. used TC method to analyze the uncertainty of AMSR-2, SMAP and SMOS, and found that the random errors among different remote sensing products were significantly inconsistent in spatial distribution[13]. ETC is a new statistical tool developed by introducing correlation coefficient on the basis of TC method. Yuan et al. used ETC method to solve the scale mismatch problem between SMAP products and ground measured data [14]. TCH was originally developed to evaluate the random error of atomic clocks, and now it is widely used to quantify the uncertainty of multiple data sets (generally more than three). For instance, Liu et al. [3] investigated the relative uncertainty of 11 soil moisture products in the Qinghai-Tibet Plateau using the TCH method. The results indicated that SMOS-IC products were notably affected by radio frequency interference, JAXA products exhibited higher air noise, and LPRM products demonstrated greater relative uncertainty in the southeast of the study area. To detect temporal non-stationary errors during uncertainty analysis, Zhou et al. (2021) proposed a triple collocation-based 2D (TC-2D) soil moisture merging methodology [15].The method combines the error variance in the temporal and spatial dimensions and achieves the merging of multiple products in a least-square framework. Although this method produces a superior merged SM product, there are some shortcomings: 1) the method operates under the assumption that all SM values share the same spatial error variance at any given time, disregarding potential variations in error variances across different regions.; 2) the method assesses spatial and temporal error variances independently, later averaging them with weighted factors. However, this post-combination approach could introduce additional uncertainty.

To address the potential issues mentioned above, this article proposes a spatial-temporal three-cornered hat (ST-TCH) method. This method analyzes the spatial-temporal uncertainty of homogeneous pixels in the neighborhood. We apply this method to four soil moisture (SM) products: AMSR2, SMAP, FY3B, and ERA-Interim. We also implement the original TCH for comparisons. Moreover, to demonstrate the enhanced accuracy achieved by our method in producing merged products, we merged the four products using three merging schemes (equal-weight, TCH-based, ST-TCH-based). Both the parent products and the merged products were validated using in-situ data collected over the Qinghai-Tibet Plateau.

2. Data sets

2.1 SMAP passive data

SMAP is a satellite launched by the National Aeronautics and Space Administration (NASA) in January 2015 for monitoring global soil moisture and landscape freeze-thaw conditions. The satellite carries both L-band active microwave radar and passive microwave radiometer, but the L-band active microwave radar ceased operation on July 7, 2015. On March 31 2015, SMAP provided L-band (1.41GHz) passive microwave remote sensing data for the first time. It’ s satellite orbit is synchronized with the sun, and the satellite's descending overpass is 6:00 LST and ascending overpass is 18:00 LST. The descending SMAP Level 3 daily passive data

(9 km) is collected from January 2015 to December 2016[16]. Data source: https://nsidc.org/data/spl3smap/versions/2.

2.2 AMSR2 passive data

AMSR2 was launched by Japan Aerospace Exploration Agency(JAXA) in 2012,which is onboard the Global Change Observation Mission–Water 1 (GCOM-W1) mission. It provides near real-time passive microwave observations at global scale with equatorial overpass times of 1:30 a.m./p.m.[17].The AMSR2 SM products are retrieved using C- and X-band brightness temperature (Tb)[18]. The SM used in this study was LPRM-AMSR2 Level-3 descending V001 Data products at 10 km spatial resolution which was retrieved by Land Parameter Retrieval Model(LPRM) Algorithm. The AMSR2 data were downloaded from https://search.earthdata.nasa.gov/.

2.3 FY3B passive data

FY-3B was successfully launched by the China National Space Administration (CNSA)on 5 November 2010.It provides the passive microwave radiometer observations called Microwave Radiation Imager (MWRI)[19] with equatorial overpass times of 1:40 a.m./p.m. The SM used in this study was 25km FY-3B level-1 with the EASE-GRID projection, which was retrieved by the inversion model based on the brightness temperature data of relevant channels. FY-3B data can be obtained from http://satell ite.nsmc.org.cn/ portalsite/default. aspx.

2.4 Reanalysis data

ERA-Interim is the global atmospheric reanalysis produced by the European Centre for Medium-Range Weather Forecasts (ECMWF)[20]. The SM used in this study was the volume of water in soil layer 1 (0-7cm) with the spatial resolution of 0.125°. ERA-Interim can be obtained from http://apps.ecmw f.int/datasets/.

2.5 In-situ data

In this paper, four ground monitoring networks of SM in Qinghai-Tibet Plateau are selected, namely Ngari, Naqu, Maqu and Pali. There are two main sources of network data of the four stations: 1) hourly observation data set of soil moisture and temperature in Qinghai-Tibet Plateau (2008-2016) (https://data.tpdc.ac.cn/zh-hans/); 2) CTP-SMTMN in International soil moisture observation Network (ISMN) (https://ismn.geo.tuwien.ac.at/en/). In this study, the point data (cm^3/cm^3) with a nominal depth of 5cm and no anomalies at 6: 00 am were selected.

3. Proposed method

For soil moisture data in the Qinghai-Tibet Plateau, spatial uncertainty of pixels can vary even on the same day across different regions. The ST-TCH method addresses this spatial heterogeneity by employing a spatial moving window. In the ST-TCH method, a moving window is utilized to construct the temporal and spatial sequence of soil moisture within the neighborhood. Similarity between the pixels in the neighborhood and the central pixel is calculated based on Spearman correlation coefficient. A threshold is set to filter out heterogeneous pixels, minimizing their interference within the window. Subsequently, the

homogeneous spatial-temporal sequence of soil moisture is vectorized in the spatial dimension. Finally, the TCH method is employed to analyze the uncertainty of the vectorized sequences within the neighborhood. The detailed process of this method is as follows:

(1) Construct the spatio-temporal sequence of soil moisture within the neighborhood by utilizing a moving window of size w×w to extract the time series of soil moisture from both the central pixel and its neighboring pixels. Given the potential spatial heterogeneity, variations between neighboring pixels and the central pixel may exist. To mitigate the interference of heterogeneous pixels within the window, it's essential to incorporate a similarity assessment process.

(2) Derive a homogeneous spatial-temporal sequence of soil moisture within the neighborhood. The Spearman correlation coefficient is utilized to assess the degree of similarity. This coefficient employs a monotonic function to evaluate the correlation between two statistical variables. The calculation formula is as follows:

$$\rho = 1 - \frac{6\sum d_i^2}{M(M^2 - 1)} \tag{1}$$

where d_i represents the difference of the rank values of the ith data pair. We utilize the Spearman correlation coefficient to calculate the similarity of time series between neighboring pixels and the central pixel. Subsequently, a threshold (ρ^*) is set to eliminate neighboring pixels below ρ^*, identifying them as heterogeneous pixels.

(3) Steps (1) and (2) are performed individually on different products. Subsequently, the homogeneous spatio-temporal series of soil moisture is vectorized in the spatial dimension to yield the spatio-temporal fusion series of various products.

(4) TCH is used to analyze the uncertainty of series of different products acquired form step (3), and the relative uncertainty (RU) of each product is obtained.

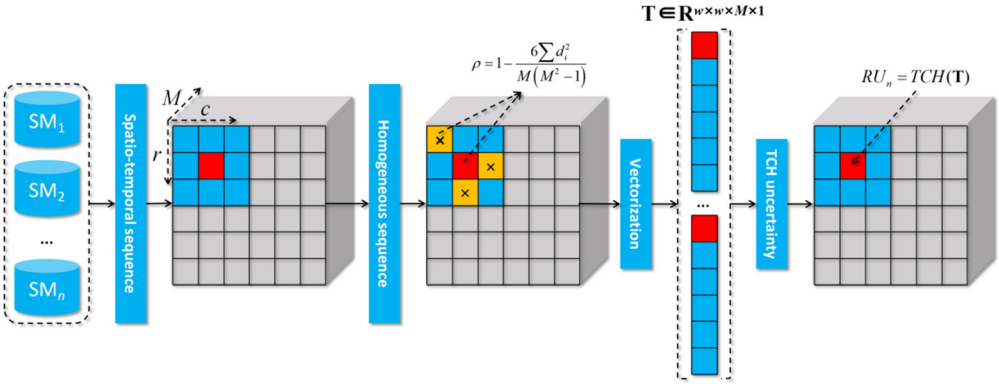

Fig. 1. The flowchart of spatial-temporal three-cornered hat.

Fig 1 illustrates the principle of the ST-TCH method proposed in this paper, while Algorithm 1 shows the pseudo code of the algorithm. The method proposed in this paper holds the

following potential advantages: 1) Reflecting the changing spatial uncertainty of soil moisture on each grid as the window moves, resulting in a more realistic representation; 2) Achieving a synchronous fusion of temporal and spatial dimensions, thereby avoiding the introduction of additional errors from separate analysis and weighted averages; 3) Taking into account the homogeneous pixel set within the neighborhood window, thus increasing the sample size of soil moisture data for uncertainty analysis.

To verify the effectiveness of the proposed ST-TCH method, four products (SMAP, AMSR2, FY-3B, and ERA-Interim) were utilized to get their relative uncertainties. The resulting relative uncertainties were then employed as weights in the merging process. The calculation for these weights was as follows:

$$\lambda_n = \frac{RU_n^{-1}}{\sum_{n=1}^{N} RU_n^{-1}} \tag{2}$$

here RU_n^{-1} represents epresents the inverse of RU_n, andλ_n represents merged weights of the different products. With these values, the merged product can be obtained

$$SM_{\text{merge}} = \sum_{n=1}^{N} \lambda_n SM_n \tag{3}$$

The four SM products are merged based on the three different SM merging schemes: 1) Equal-weight Merging: This simple reference scheme assigns equal weights (i.e., 1/4) to each SM product; 2) TCH Merging: In this scheme, the Relative Uncertainties (RU) obtained by TCH were utilized as weights following Eq. (2) and Eq. (3); 3) ST-TCH merging, the same as scheme 2), but the RU was obtained through the ST-TCH method. Furthermore, the merged products was evaluated through direct comparison with independent in-situ SM observations, using the Pearson correlation coefficient (R) values.

Algorithm 1: Spatial-temporal three-corned hat (ST-TCH).

Input: N SM products $\{SM\}_n$ (n=1, 2, ..., N), The size of each product is $R^{r\times c\times M}$,r is the size of row,c is the size of column, M is the length of time series， discrimination threshold of heterogeneous pixels in neighborhood $\rho*$

Output: Relative uncertainty of space-time integration for N products $\{Spa\text{-}temp_n\}$

Initialization: Mirror fill each image with window size $w\times w$, the size of the filled image becomes (r+2×w,c+2×w)

Main loop:

For i from (w+1) to (w+r)

  For j from (w+1) to (w+c)

    $T_{n,p}=SM_n(i\pm p, j\pm p,:)$, p = 1, 2, ..., ($w$-1)/2

    $T_{n,center}=SM_n(i,j,:)$

    $T_{n,zeros}$ = zeros(1,1,M)

    Calculate ρ according to（1）

$$T_n = \begin{cases} [T_{n,center}; T_{n,p}] & if\ \rho > \rho^* \\ [T_{n,center}; T_{n,zeros}] & esle \end{cases}$$

$T=[T_1, T_1, ..., T_N,]$

$\mathrm{RU}_n^{\mathrm{ST}} = \mathrm{TCH}(\mathrm{T})$

$Spa\text{-}temp_n(i,j) = \mathrm{RU}_n^{\mathrm{ST}}$

End for

End for

Return $\{Spa\text{-}temp_n\}$

4. Experimenal results

4.1 Parameter Sensitive Analysis and Ablation Study

To determine the optimal window size (w) and the threshold (ρ^*), we set w to 3, 5, and 7, and ρ^* to 0.5, 0.6, 0.7, 0.8, and 0.9. Using these parameter combinations, spatial-temporal sequence data were obtained from the four products with a data size of $(M \times w^2) \times 4$. This sequence data was then input into TCH to calculate the relative uncertainties of the four products. R values for different combinations of parameters were obtained by regression analysis with the in-situ data.

As shown in Fig. 2, under the same threshold ρ^*, R becomes lower as w increases and is highest when w=3. Under the same window size w, R generally decrease as ρ^* increases, being highest when ρ^*=0.9. Consequently, the optimal parameters identified for the subsequent experiments were w=3 and ρ^*=0.9. The results denote that the method proposed in this paper works best with smaller window size (w) and higher threshold (ρ^*).

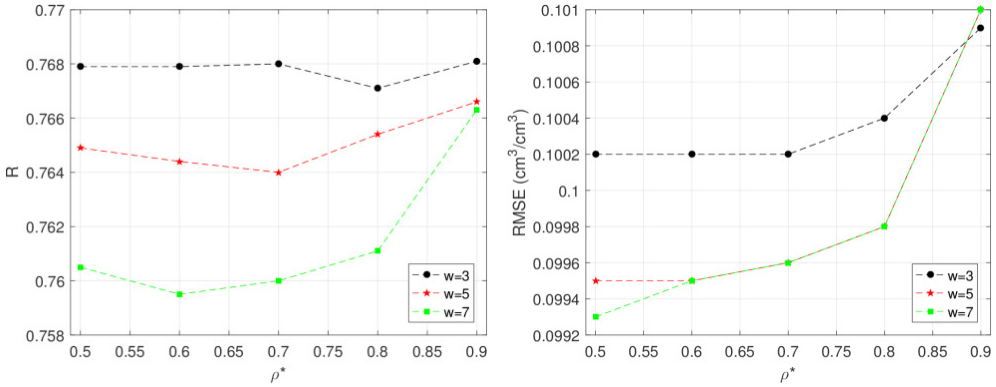

(a) R (b) RMSE

Fig. 2 The impact of window size and threshold on ST-TCH (Optimal: w=3, ρ*=0.9).

4.2 Comparison of relative uncertainties

To visually assess the spatial impact of different uncertainty methods, we compared and analyzed the relative uncertainties generated by TCH and ST-TCH in our experiment. As depicted in Figure 3, ST-TCH and TCH exhibit high similarity in most areas, indicating that temporal uncertainty plays a predominant role. Relative to TCH, ST-TCH provides a more comprehensive spatial distribution of RU. When comparing the results across different products, it becomes apparent that SMAP and ERA-Interim exhibit low relative uncertainties, whereas AMSR2 displays variable relative uncertainties across space.

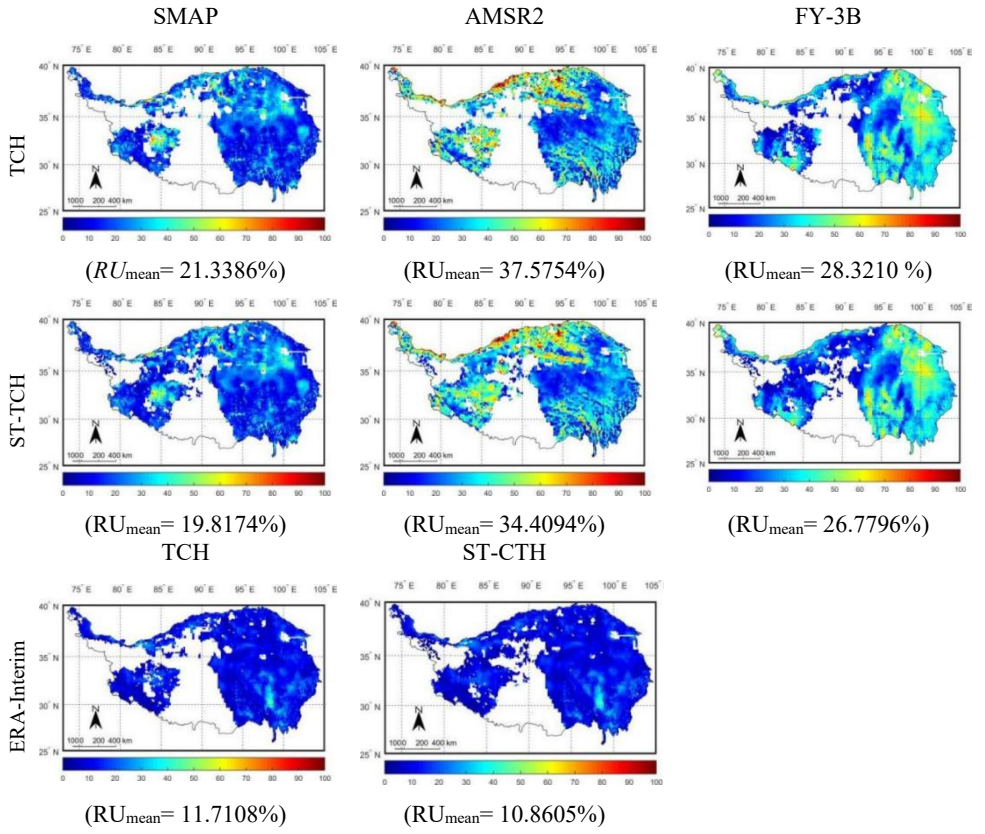

Fig. 3 Spatial map of relative uncertainties for four SM products

4.3 Evaluation results of parent and merging SM products

Table 1. The results of direct evaluation using in-situ data

Products	R	RMSE	bias	ubRMSE
SMAP	0.7519	**0.0593**	**-0.0282**	0.0521
AMSR2	0.7156	0.1084	-0.0933	0.0552
FY3B	0.2323	0.1264	-0.0873	0.0915
ERA-Interim	0.4619	0.1417	-0.1252	0.0665

EM	0.7641	0.0976	-0.0843	**0.0493**
TM	0.7671	0.1020	-0.0890	0.0499
STM (Ours)	**0.7688**	0.1009	-0.0877	0.0499

As shown in Fig. 4, parent and merged soil moisture products are directed evaluated using in-situ data, and the accuracy of different soil moisture products is shown in Table 1. The R value of FY3B, among the original products, is the lowest, and it has a relatively large RMSE compared to the in-situ data. The R value of the fused soil moisture product is higher than that of the parent products, which shows that the correlation between the product and the measured data is improved after fusion. Compared with other fusion methods, the fusion method based on ST-TCH (the method in this paper) has achieved higher R value. This may indicates that merged products through comprehensive consideration of both temporal and spatial uncertainty are expected to further reduce the uncertainty of the products.

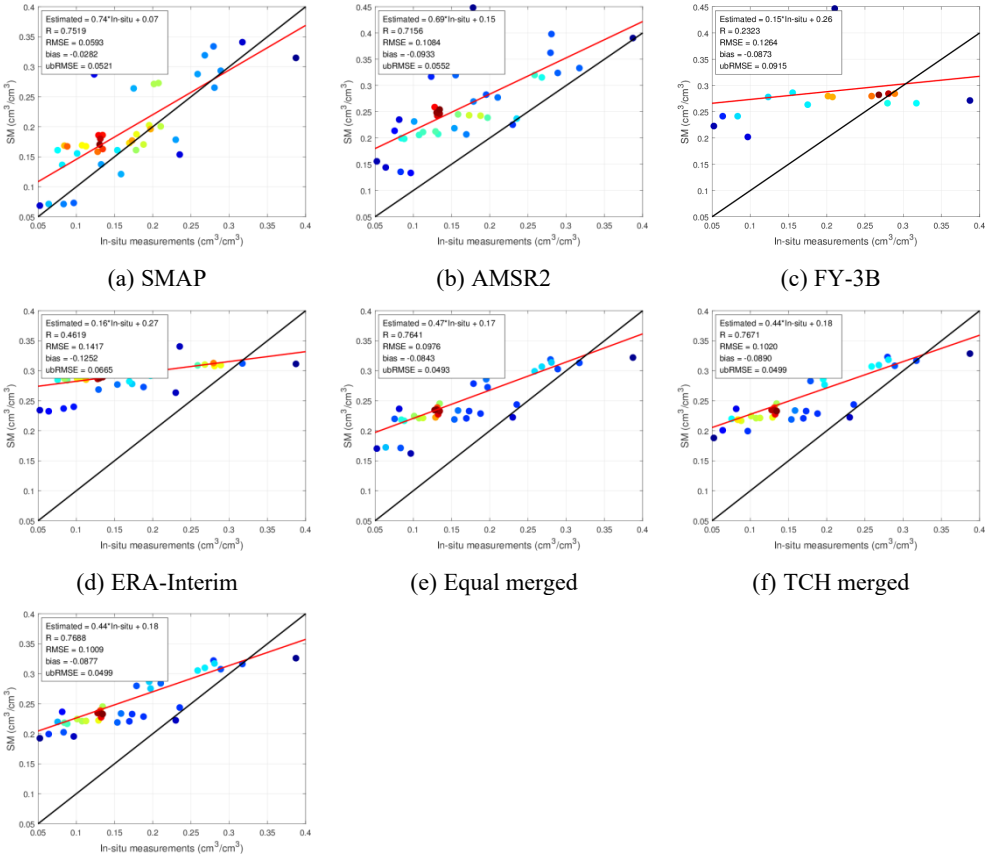

(a) SMAP (b) AMSR2 (c) FY-3B

(d) ERA-Interim (e) Equal merged (f) TCH merged

(g) ST-TCH merged (Ours)

Fig. 4 Scatterplots of different products compared with in-situ data.

5. Conclusion

In this study, we introduced a spatial-temporal three-cornered hat method for analyzing the uncertainty of soil moisture products. Our sensitivity analysis indicates that this method is more effective with a smaller window size and a larger discriminant threshold. When comparing the spatial distribution of Relative Uncertainties (RU) and merged products obtained by ST-TCH (the proposed method) with the original TCH method, the results demonstrate that the relative uncertainties obtained by ST-TCH have a more compre- hensive spatial distribution. Furthermore, the merged products based on ST-TCH achieve the highest R-values among all products. The ST-TCH method shows notable improvements owing to the potential advantages mentioned in Section III. As a result, ST-TCH effectively addresses the limitation of TCH in neglecting spatial heterogeneity. This probably makes it a valuable tool for uncertainty analysis of soil moisture products and multi-product merging research.

Acknowledgments: This work was supported in part by the National Natural Science Foundation of China under Grant 42201406, Grant 41971279, and Grant 42271324, in part by the Natural Science Foundation of Jiangsu Province under Grant BK20221506, and in part by the Natural Science Foundation of the Jiangsu Higher Education Institutions of China under Grant 22KJD420001.

References

[1] C.-H. Su, D. Ryu, W. T. Crow, and A. W. Western, "Stand-alone error characterisation of microwave satellite soil moisture using a Fourier method," *Remote Sens. Environ.,* vol. 154, pp. 115-126, Apr. 2014.

[2] C.-H. Su, D. Ryu, A. W. Western, and W. Wagner, "De-noising of passive and active microwave satellite soil moisture time series," *Geophys. Res. Lett.,* vol. 40, no. 14, pp. 3624-3630, Jun. 2013.

[3] J. Liu, L. Chai, J. Dong, D. Zheng, J. P. Wigneron, S. Liu, J. Zhou, T. Xu, S. Yang, Y. Song, Y. Qu, and Z. Lu, "Uncertainty analysis of eleven multisource soil moisture products in the third pole environment based on the three-corned hat method," *Remote Sens. Environ.,* vol. 255, pp. 112225, 2021.

[4] A. Gruber, G. De Lannoy, C. Albergel, A. Al-Yaari, L. Brocca, J. C. Calvet, A. Colliander, M. Cosh, W. Crow, W. Dorigo, C. Draper, M. Hirschi, Y. Kerr, A. Konings, W. Lahoz, K. McColl, C. Montzka, J. Muñoz-Sabater, J. Peng, R. Reichle, P. Richaume, C. Rüdiger, T. Scanlon, R. van der Schalie, J. P. Wigneron, and W. Wagner, "Validation practices for satellite soil moisture retrievals: What are (the) errors?," *Remote Sens. Environ.,* vol. 244, pp. 111806, 2020.

[5] A. Stoffelen, "Toward the true near-surface wind speed: Error modeling and calibration using triple collocation," *J. Geophys. Res.: Oceans,* vol. 103, no. C4, pp. 7755-7766, 1998.

[6] A. Gruber, W. A. Dorigo, W. Crow, and W. Wagner, "Triple Collocation-Based Merging of Satellite Soil Moisture Retrievals," *IEEE Trans. Geosci. Remote Sens.,* vol. 55, no. 12, pp. 6780-6792, Dec 2017.

[7] A. Gruber, C. H. Su, S. Zwieback, W. Crow, W. Dorigo, and W. Wagner, "Recent advances in (soil moisture) triple collocation analysis," *Int. J. Appl. Earth Obs. Geoinf.,* vol. 45, pp. 200-211, 2016.

[8] X. Wu, Q. Xiao, J. Wen, and D. You, “Direct Comparison and Triple Collocation: Which Is More Reliable in the Validation of Coarse-Scale Satellite Surface Albedo Products,” *J. Geophys. Res.: Atmos.,* vol. 124, no. 10, pp. 5198-5213, 2019.
[9] K. A. McColl, J. Vogelzang, A. G. Konings, D. Entekhabi, M. Piles, and A. Stoffelen, “Extended triple collocation: Estimating errors and correlation coefficients with respect to an unknown target,” *Geophys. Res. Lett.,* vol. 41, no. 17, pp. 6229-6236, 2014.
[10] P. Tavella, and A. Premoli, “Estimating the Instabilities of N Clocks by Measuring Differences of their Readings,” *Metrologia,* vol. 30, no. 5, pp. 479, 1994/01/01 1994.
[11] T. Rieckh, and R. Anthes, “Evaluating two methods of estimating error variances using simulated data sets with known errors,” *Atmos. Meas. Tech.,* vol. 11, no. 7, pp. 4309-4325, 2018.
[12] J. Vogelzang, and A. Stoffelen, “Quadruple Collocation Analysis of In-Situ, Scatterometer, and NWP Winds,” *J. Geophys. Res.: Oceans,* vol. 126, no. 5, 2021.
[13] S. Wang, W. Liu, and L. Liang, “Uncertainty Analysis and Data Fusion of Microwave Remote Sensing Soil Moisture Products based on Triple-Collocation Method,” *Remote Sensing Technology and Application,* vol. 34, no. 6, pp. 1227-1234, 2019.
[14] Q. Yuan, H. Xu, T. Li, H. Shen, and L. Zhang, “Estimating surface soil moisture from satellite observations using a generalized regression neural network trained on sparse ground-based measurements in the continental U.S,” *J. Hydrol.,* vol. 580, pp. 124351, 2020.
[15] J. Zhou, W. T. Crow, Z. Wu, J. Dong, H. He, and H. Feng, “A triple collocation-based 2D soil moisture merging methodology considering spatial and temporal non-stationary errors,” *Remote Sens. Environ.,* vol. 263, pp. 112509, 2021.
[16] P. E. O'Neill, S. Chan, E. G. Njoku, T. Jackson, R. Bindlish, and J. Chaubell, 2020. “ L3 Radiometer Global Daily 36 km EASE-Grid Soil Moisture, Version 7,” Boulder, Colorado USA. NASA National Snow and Ice Data Center Distributed Active Archive Center, https://doi.org/10.5067/HH4SZ2PXSP6A.
[17] B. Fang, V. Lakshmi, R. Bindlish, and T. J. Jackson, “AMSR2 Soil Moisture Downscaling Using Temperature and Vegetation Data,” *Remote Sens.,* vol. 10, no. 10, Oct 2018.
[18] K. Imaoka, M. Kachi, H. Fujii, H. Murakami, M. Hori, A. Ono, T. Igarashi, K. Nakagawa, T. Oki, Y. Honda, and H. Shimoda, “Global Change Observation Mission (GCOM) for Monitoring Carbon, Water Cycles, and Climate Change,” *Proc. IEEE,* vol. 98, no. 5, pp. 717-734, May 2010.
[19] Y. K. Cui, X. Chen, W. T. Xiong, L. He, F. Lv, W. J. Fan, Z. L. Luo, and Y. Hong, “A Soil Moisture Spatial and Temporal Resolution Improving Algorithm Based on Multi-Source Remote Sensing Data and GRNN Model,” *Remote Sens.,* vol. 12, no. 3, Feb 2020.
[20] L. L. Ge, R. L. Hang, Y. Liu, and Q. S. Liu, “Comparing the Performance of Neural Network and Deep Convolutional Neural Network in Estimating Soil Moisture from Satellite Observations,” *Remote Sens.,* vol. 10, no. 9, Sep 2018.